SLAC–PUB–95-6836
July 1995

Anisotropies in Strain and Quantum Efficiency of Strained GaAs grown on GaAsP*

R. A. Mair and R. Prepost

Department of Physics, University of Wisconsin, Madison, Wisconsin 53706

H. Tang, E. L. Garwin, T. Maruyama and G. Mulhollan

Stanford Linear Accelerator Center,

Stanford University, Stanford, California 94309

Abstract

An anisotropy in the quantum efficiency (QE) has been observed in photoemission from strained GaAs photocathodes excited by linearly polarized light. The wavelength dependence of the anisotropy is closely correlated with that of the electron-spin polarization. Based on a theoretical analysis, we show that the QE anisotropy is caused by an in-plane strain anisotropy arising from anisotropic strain relaxation. The QE anisotropy calculated from the in-plane strain anisotropy measured with X-ray diffraction and the measured QE anisotropy are in good agreement.

Submitted to Physical Review Letters

Since the first observation of electron-spin enhancement in photoemission from a strained InGaAs layer epitaxially grown on a GaAs substrate, [1] polarized electron photoemission

* This work was supported in part by the U. S. Department of Energy under contract numbers DE-AC03-76SF00515 (SLAC), and DE-AC02-76ER00881 (UW).

from strained heterostructures has been of much research interest [2]. The polarization enhancement is a result of strain-induced splitting between heavy- and light-hole valence bands which permits optical excitation from a single band, leading potentially to 100% polarization of the photoemitted electrons. Photocathodes based on strained GaAs grown on $GaAs_{1-x}P_x$ have been incorporated in the polarized electron source [3] at the Stanford Linear Accelerator Center (SLAC), producing high intensity electron beams with polarization over 80% for high energy physics experiments [4].

When a lattice-mismatched layer is grown on a substrate, the misfit is accommodated by elastic strain in the epitaxial layer and pseudomorphic growth takes place. However, if the epitaxial layer exceeds a critical thickness, the stored elastic strain in the epitaxial layer is relieved by misfit dislocations. For the zinc-blende structure, misfit dislocations develop asymmetrically along the two orthogonal directions [110] and $[1\bar{1}0]$, resulting in an anisotropic strain within the plane of the epitaxial layer [5]. This letter reports the first systematic study of the effects of strain anisotropy on quantum efficiency (QE) using samples with a heterojunction of GaAs epitaxially grown on a $GaAs_{1-x}P_x$ buffer layer. A range of strains was studied by using samples with varying epitaxial layer thickness and varying buffer layer phosphorus concentrations. For these samples the lattice strains along the [110] and $[1\bar{1}0]$ directions were measured using double crystal X-ray diffraction, and the electron spin polarization and QE were measured as a function of excitation photon wavelength.

The relationship between the in-plane strain anisotropy and the observed QE anisotropy may be understood by considering the effect of shear on the electron wave functions of the valence bands. In the absence of any strain, the valence band wave functions for electrons in the vicinity of Γ have the symmetry of atomic p-like $|J, m_j\rangle$ states. The heavy-hole, light-hole and split-off valence bands correspond to $|\frac{3}{2}, \pm\frac{3}{2}\rangle$, $|\frac{3}{2}, \pm\frac{1}{2}\rangle$, and $|\frac{1}{2}, \pm\frac{1}{2}\rangle$, respectively. The effect of strain on the band structure is described in terms of the strain tensor ϵ_{ij} [6] by the orbital-strain Hamiltonian:

$$H = -a\epsilon - 3b \times [(L_x^2 - \frac{1}{3}\mathbf{L}^2)\epsilon_{xx} + \text{c.p.}] - \frac{6d}{\sqrt{3}}[\{L_x L_y\}\epsilon_{xy} + \text{c.p.}], \qquad (1)$$

where $\epsilon = (\epsilon_{xx} + \epsilon_{yy} + \epsilon_{zz})$, $\mathbf{L}$ is the angular momentum operator, a, b, and d are deformation potentials [7], $\{L_x L_y\} = \frac{1}{2}(L_x L_y + L_y L_x)$, and c.p. denotes cyclic permutation with respect to x, y and z. For the case of lattice mismatched epitaxial growth on (001) surfaces, the strain is ideally a pure biaxial compression represented by a strain tensor with only diagonal elements. The electron wave functions at Γ are still the $|J, m_j\rangle$ states, but the normally degenerate heavy-hole and light-hole bands are now split by an amount proportional to the induced strain. The quantization axis ($\hat{z}$) is oriented along the effective uniaxial strain ([001] in this case). These wavefunctions are x-y symmetric, precluding any QE anisotropy.

If a small in-plane shear (ϵ_{xy}) is present, the wave functions at Γ are perturbed to first order as:

$$|\frac{3}{2}, \pm\frac{3}{2}\rangle \Rightarrow |\frac{3}{2}, \pm\frac{3}{2}\rangle \mp \frac{id \cdot \epsilon_{xy}}{E_{hh} - E_{lh}} |\frac{3}{2}, \mp\frac{1}{2}\rangle + \frac{i\sqrt{2}d \cdot \epsilon_{xy}}{E_{hh} - E_{so}} |\frac{1}{2}, \mp\frac{1}{2}\rangle \tag{2a}$$

$$|\frac{3}{2}, \pm\frac{1}{2}\rangle \Rightarrow |\frac{3}{2}, \pm\frac{1}{2}\rangle \pm \frac{id \cdot \epsilon_{xy}}{E_{hh} - E_{lh}} |\frac{3}{2}, \mp\frac{3}{2}\rangle, \tag{2b}$$

where E_{hh}, E_{lh}, and E_{so} are the Γ point energies of the heavy-hole, light-hole, and split-off valence bands. The strain dependent energy splittings are $E_{hh} - E_{lh} = -2b(\frac{C_{11}}{2C_{12}} + 1)\epsilon_{zz}$ and $E_{hh} - E_{so} = \frac{E_{hh} - E_{lh}}{2} + \Delta$, where Δ is the spin-orbit splitting, and C_{11}, C_{12} are elastic stiffness constants. The shear strain will mix the heavy-hole and light-hole/split-off valence states and affect the optical transition probabilities from the various valence bands to the conduction band. However, since the mixing occurs only between opposite sign m_j states, if the excitation light is 100% circularly polarized, only one state can be excited and the electron-spin polarization will be unaffected (to first order in ϵ_{xy}). On the other hand, if the excitation light is linearly polarized, more than one state can be excited and the excitation probabilities will be dependent on the direction of linear polarization relative to a reference axis. Define the QE anisotropy:

$$\frac{\Delta QE}{QE}(\phi) \equiv \frac{QE(\phi) - QE(\phi + \frac{\pi}{2})}{QE(\phi) + QE(\phi + \frac{\pi}{2})} \tag{3}$$

where $QE(\phi)$ is the quantum efficiency for the angle ϕ of the linear polarization relative to a reference axis. The dipole operator appropriate for linearly polarized light traveling along

$\hat{z}$ is expressed as $X\cos\phi + Y\sin\phi$, and the QE anisotropy is calculated with the assumption that the sole dependence is on the dipole matrix elements between the perturbed valence bands and the conduction band. The resulting QE anisotropies for transitions from the perturbed heavy hole and light hole valence bands calculated separately are:

$$\frac{\Delta QE}{QE}(\phi)\Big|_{hh} = \frac{2(\delta_1+\delta_2)\sin 2\phi}{(1+(\delta_1+\delta_2)^2)} \;\cong\; 2(\delta_1+\delta_2)\sin 2\phi \tag{4a}$$

$$\frac{\Delta QE}{QE}(\phi)\Big|_{lh} = \frac{-6\delta_1\sin 2\phi}{(1+{\delta_1}^2)} \;\cong\; -6\delta_1\sin 2\phi, \tag{4b}$$

where $\delta_1 = d\cdot\epsilon_{xy}/(\sqrt{3}(E_{hh}-E_{lh}))$ and $\delta_2 = 2d\cdot\epsilon_{xy}/(\sqrt{3}(E_{hh}-E_{so}))$. The QE anisotropies for heavy hole and light hole transitions are opposite in sign such that when both transitions are being pumped, the anisotropy is less than for the case of heavy hole pumping only. The QE anisotropy magnitude is a maximum when $\sin(2\phi) = \pm 1$ and the expected values may be calculated in terms of the parameters in Eq. (4).

The wavelength dependence of both electron polarization and QE anisotropy may be considered a manifestation of the wavelength dependence of the relative rates of heavy hole and light hole transitions. In this manner, the QE anisotropy corresponding to $\sin(2\phi) = 1$ is expressed as $\frac{\Delta QE}{QE}(\lambda) = \left(\frac{\Delta QE}{QE}{}^{max}_{hh}\cdot I_{hh}(\lambda) + \frac{\Delta QE}{QE}{}^{max}_{lh}\cdot I_{lh}(\lambda)\right)/(I_{hh}(\lambda)+I_{lh}(\lambda))$ where I_{hh}, I_{lh} are the overall heavy hole and light hole transition rates. Similarly, under circularly polarized pump conditions, the electron polarization will be given by $P_e(\lambda) = R(I_{hh}(\lambda) - I_{lh}(\lambda))/(I_{hh}(\lambda)+I_{lh}(\lambda))$. Here, electron polarizations of $\pm 100\%$ are used for heavy hole / light hole transitions respectively. The term R accounts for any spin relaxation within the crystal or at the surface and is assumed to be wavelength independent. Combining these two relations with eq. (4), we obtain

$$\frac{\Delta QE}{QE}(\lambda) = 2\delta_1(2\frac{P_e(\lambda)}{R} - 1) + \delta_2(\frac{P_e(\lambda)}{R} + 1), \tag{5}$$

which shows that the QE anisotropy and electron polarization are related in a simple linear fashion.

The strained samples for the present experiment were grown by the Spire Corporation [8] using Metal-Organic-Chemical-Vapor-Deposition (MOCVD), and consisted of GaAs epitax-

ial layers grown on a $GaAs_{1-x}P_x$ buffer layer. A detailed description of the sample structures is given in Maruyama et al. [2] All the samples show cross hatch-marks on the surface due to strain relaxation in the $GaAs_{1-x}P_x$ buffer layer. The hatch-marks were observed to be predominantly along the $[1\bar{1}0]$ direction and were used to orient the crystal for X-ray diffraction and QE anisotropy measurements. Table 1 shows the active GaAs layer thickness (t) and phosphorus fraction (x) of the $GaAs_{1-x}P_x$ buffer of the samples used for the experiment.

The lattice structure of the strained GaAs layer for each of the samples was analyzed with a double-crystal x-ray diffractometer. The diffractometer uses CuK_α radiation together with a four-crystal Ge(220) monochromator and either a slit with a 2θ acceptance angle of $0.15°$ or a Ge(220) analyzer crystal (triple axis diffractometry). Reciprocal lattice maps were taken to locate the epitaxial GaAs peak relative to the GaAs substrate peak by performing a series of ω-2θ scans, simultaneous rotations of the sample (ω) and detector (2θ), for different ω offsets [9]. Symmetric Bragg reflections (004) and asymmetric reflections, (113) or (224), were used to measure the lattice constant $a_\perp$ along [001], and two lattice constants $a_{\|}^{[110]}$ and $a_{\|}^{[1\bar{1}0]}$ along [110] and $[1\bar{1}0]$. Any difference in $a_{\|}^{[110]}$ and $a_{\|}^{[1\bar{1}0]}$ constitutes an in-plane shear strain which is calculated by $\epsilon_{xy} = (a_{\|}^{[110]} - a_{\|}^{[1\bar{1}0]})/(a_{\|}^{[110]} + a_{\|}^{[1\bar{1}0]})$. The misfit strain along [001] represents the desired tetragonal distortion and is calculated by $\epsilon_{zz} = (a_\perp - a_0)/a_0$, where a_0 is the GaAs lattice constant. The measured strain components, ϵ_{zz} and ϵ_{xy}, for the six samples are given in Table 1.

The QE anisotropy and electron polarization were measured in a UHV cathode test system equipped with a load-lock for cathode introduction/removal and a compact medium-energy (20-30 kV) retarding-field Mott detector for polarization measurements. A white light source coupled to a monochromator served as an optical pump variable over the desired wavelength range (700 nm – 900 nm) for the spectral studies. The combination of an electronically controlled liquid crystal variable phase retarder and a cube polarizer allowed for easy control of the polarization state of the light. The cathode was activated to obtain a negative-electron-affinity surface using a cesium channel dispenser and a nitrogen trifluoride leak source. the decay time of the QE was typically in excess of 200 hours.

The sequence of the electron polarization and QE anisotropy measurements was as follows. After a cathode activation, the electron polarization was first measured with circularly polarized light as a function of wavelength. With the wavelength fixed at the value corresponding to the maximum electron polarization, the QE anisotropy for two orthogonal linear polarization states of the excitation light was measured as a function of the angle between the light polarization direction and the [100] axis of the sample (see Eq. (3)). The angle ϕ was varied by rotating the polarizer/phase-retarder assembly. Since the two linear polarization states for each angle were realized by electronically varying the amount of phase retardation, the light intensity remained constant and systematic errors due to unwanted beam steering were minimized. Finally, the QE anisotropy was measured as a function of the excitation wavelength while the linear polarization angle ϕ was fixed at the value which yielded the maximum QE anisotropy.

The QE anisotropy and polarization measurements were performed for all six samples. Fig. 1 shows the QE anisotropy $\frac{\Delta QE}{QE}$ for sample 3 as a function of the azimuthal angle of the linear polarization axis relative to the [100] direction measured at a wavelength $\lambda = 865$ nm. Two features are immediately evident. First, the variation in $\frac{\Delta QE}{QE}$ as a function of ϕ is sinusoidal with a periodicity of 180°. Secondly, the maximum $\frac{\Delta QE}{QE}$ value occurs at $\phi = 135°$, implying that the maximum and minimum QE for linearly polarized light correspond to the $[1\bar{1}0]$ and [110] axes, respectively [10]. The solid line in Fig. 1 represents the best fit of a 180° periodicity sine wave to the data. The good agreement between these results and the theoretical predictions confirms that the observed QE anisotropy is caused by an in-plane strain anisotropy along the [110] and $[1\bar{1}0]$ directions.

Fig. 2 shows the maximum QE anisotropy and electron-spin polarization for sample 3 as a function of wavelength. While the two curves are arbitrary scaled, their overall shapes bear a striking similarity. As the wavelength exceeds a critical value (about 800 nm in this case) such that the excitation from the light-hole band is preferentially suppressed with respect to that from the heavy-hole band, both the QE anisotropy and polarization increase until reaching their respective maxima at about 860 nm. The inset in Fig. 2 shows the

maximum QE anisotropy plotted against the corresponding measured electron polarization in the wavelength range from 740 - 850 nm. The correlation between the QE anisotropy and polarization is observed to be linear in accord with the prediction of Eq. (5). The solid line in the inset is a best fit straight line to the points. Both the polarization and QE anisotropy show a monotonic decrease for excitation wavelengths longer than about 860 nm. While the origin of this decrease is not known, it may be due to electrons emitted from states other than the valence band, such as surface states and acceptor states.

The strain components measured by X-ray diffraction may be used to calculate an expected maximum QE anisotropy using Eq. (4a), assuming the transitions are primarily from heavy-hole to conduction band. In this manner, the values for the expected QE anisotropy have been calculated for the six samples and are shown in column 8 of Table 1 [11]. The indicated errors are the contributions from the measurements of ϵ_{xy}. Given the additional uncertainty of about 10% in the deformation potentials, a reasonable agreement between the observed (column 5) and expected (column 8) QE anisotropies is seen. It is expected that that the thicker, less strained samples should show lower QE anisotropies than expected from Eq. (5a) since the condition of exclusive heavy hole pumping may not be fully met.

Another interesting aspect of the strain anisotropy observed in this experiment is the dependence on the degree of strain relaxation in the sample. The maximum possible strain for a given sample is taken as the value corresponding to an epilayer in-plane lattice constant equivalent to that of the $GaAs_{1-x}P_x$ layer. The relaxation is then defined as the difference between the measured strain and the maximum possible strain. Fig. 3 shows the measured shear ϵ_{xy} plotted against the degree of relaxation together with the observed QE anisotropies. For small relaxations, the generated shear appears proportional to the degree of relaxation. At some point however, the anisotropic relaxation ceases and there is movement towards an in-plane symmetric strain. This possibly indicates that at a certain dislocation density the more relaxed of the two crystalline directions experiences a suppression in further relaxation while the other direction continues to relax. The QE anisotropy is also seen to increase with relaxation until reaching a maximum (approximately 14% here) and then decreases for

larger relaxations.

In conclusion, we have observed anisotropies in QE in photoemission from strained GaAs photocathodes optically pumped with linearly polarized light. The QE anisotropy is explained as a valence band mixing phenomenon caused by an in-plane shear strain which develops during partial relaxation of the layer. The sinusoidal nature, dependence on shear, and wavelength dependence of the QE anisotropy are all well understood in the context of the described band mixing. The existence of such a QE anisotropy in strained layer photocathodes used for polarized electron sources may lead to spin dependent intensity variations if there exists a small, unintentional, linear component in the circularly polarized pump beam.

We thank Dr. G. Waychunas of Stanford University for many helpful discussions on X-ray diffraction. We also thank G. Zapalac for many helpful discussions. This work was supported in part by the U.S. Department of Energy, under Contract Nos. DE-AC03-76SF00515 (SLAC), and DE-AC02-76ER00881 (UW).

REFERENCES

[1] T. Maruyama, E. L. Garwin, R. Prepost, G. H. Zapalac, J. S. Smith, and J. D. Walker, Phys. Rev. Lett. **66**, 2376 (1991).

[2] T. Nakanishi *et al.*, Phys. Lett. A **158**, 345 (1991); T. Maruyama, E. L. Garwin, R. Prepost, and G. H. Zapalac, Phys. Rev. **B46**, 4261 (1992); H. Aoyagi *et al.*, Phys. Lett. **A167**, 415 (1992); T. Saka *et al.*, Jpn. J. Appl. Phys. **32**, L1837 (1993); J. C. Grobli *et al.*, Phys. Rev. Lett. **74**, 2106 (1995).

[3] R. Alley *et al.*, SLAC-PUB-6489

[4] K. Abe *et al.*, Phys. Rev. Lett. **73**, 25 (1994); K. Abe *et al.*, Phys. Rev. Lett. **74**, 346 (1995).

[5] M. S. Abrahams *et al.*, Appl. Phys. Lett. **21**, 185 (1972); K. L. Kavanagh *et al.*, J. Appl. Phys. **64**, 4843 (1988); M. Grundmann, *et al.*, J. Vac. Sci. Technol. **B8**, 751 (1990); A. Bensaada *et al.*, J. Crystal Growth **130**, 433 (1993).

[6] The strain tensor ϵ_{ij} is defined as $\epsilon_{ij} = \frac{1}{2}(\frac{\partial u_i}{\partial x_j} + \frac{\partial u_j}{\partial x_i})$ where $u(x)$ is the displacement vector of a point due to strain.

[7] G. Pikus and G. Bir, Sov. Phys.-Solid State **1**, 1502 (1959); H. Hasegawa, Phys. Rev. **129**, 1029 (1963); H. Asai and K. Oe, J. Appl. Phys. **54**, 2052 (1983).

[8] Spire Corporation, Bedford, Massachusetts, 01730, USA.

[9] The reciprocal lattice mapping is described in, for example, P. F. Fewster, Appl. Surf. Sci. **50** 9, 1991.

[10] This statement is true to within $\pm 5°$ as the direction of the [110] or [1$\bar{1}$0] direction was determined only to within $\pm 5°$.

[11] The parameter values used were: Δ=340 meV, C_{11}=11.9$\times 10^{11}$dyn/cm^2, C_{12} = 5.37$\times 10^{11}$ dyn/cm^2 from: *Semiconductors*, New Series III/17a of *Landolt-Börnstein*,

edited by O. Madelung (Springer-Verlag, New York, 1982) and $b = -2.07$ eV, $d = -6.05$ eV. The values for b and d are weighted averages obtained from: F. H. Pollak et al., Phys. Rev. Lett. **16**, 942 (1966); F. H. Pollak et al., Phys. Rev. **172**, 816 (1968); and I. Balslev, *ibid.*, **177**, 1173 (1969).

FIGURES

FIG. 1. QE anisotropy as a function of azimuthal angle of the polarization axis relative to the [100] direction for sample 3.

FIG. 2. QE anisotropy and electron-spin polarization as a function of excitation light wavelength for sample 3. The two curves are arbitrary scaled.

FIG. 3. Measured shear strain (ϵ_{xy}) and QE anisotropy as a function of strain relaxation.

TABLES

TABLE I. Properties of the six measured samples described in the text. The thickness of the strained epitaxial layer is denoted by t, and x is the P fraction in the $GaAs_{1-x}P_x$ buffer layer. Columns 4-7 are measured quantities. Column 8 is the expected value of the heavy-hole QE anisotropy computed from the measured shear strain ϵ_{xy} and Eq. (4a).

Sample	t (nm)	x	Max. Pol (%)	$\Delta QE/QE$ (%)	$\epsilon_{zz}(\times 10^{-3})$	$\epsilon_{xy}(\times 10^{-3})$	$(\Delta QE/QE)_{expected}$ (%)
1	100	0.274	78.5 ±1.5	5.4 ±.5	7.07	0.32 ±.09	4.8 ±1.4
2	100	0.335	80.1 ±0.8	14.6 ±.5	6.86	0.76 ±.04	11.7 ±0.6
3	200	0.243	74.1 ±0.9	9.4 ±.5	5.68	0.47 ±.09	8.4 ±1.6
4	300	0.233	71.5 ±1.0	14.2 ±.5	4.16	0.76 ±.03	17.6 ±0.7
5	300	0.252	56.5 ±0.9	4.4 ±.5	3.82	0.40 ±.03	10.0 ±0.8
6	500	0.268	57.2 ±0.7	6.7 ±.5	1.59	0.09 ±.09	4.9 ±4.9

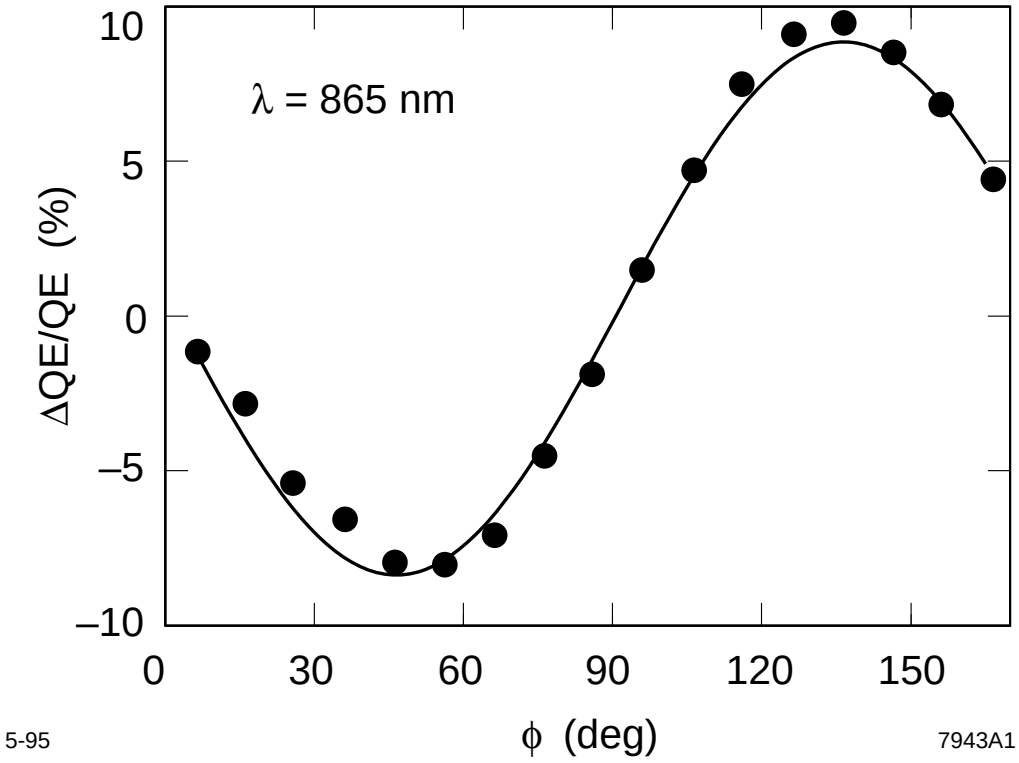

Figure 1:

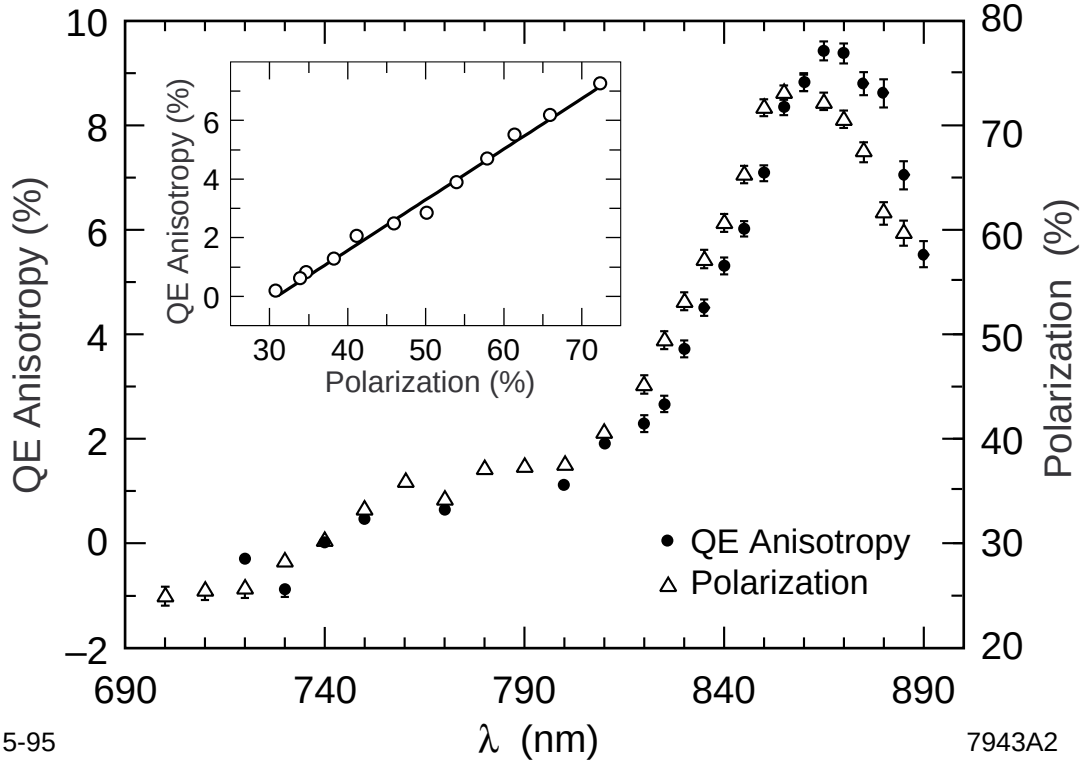
QE Anisotropy (%)
Polarization (%)
λ (nm)
QE Anisotropy
Polarization
690
740
790
840
890
10
8
6
4
2
0
–2
80
70
60
50
40
30
20
30
40
50
60
70
0
2
4
6
5-95
7943A2

Figure 2:

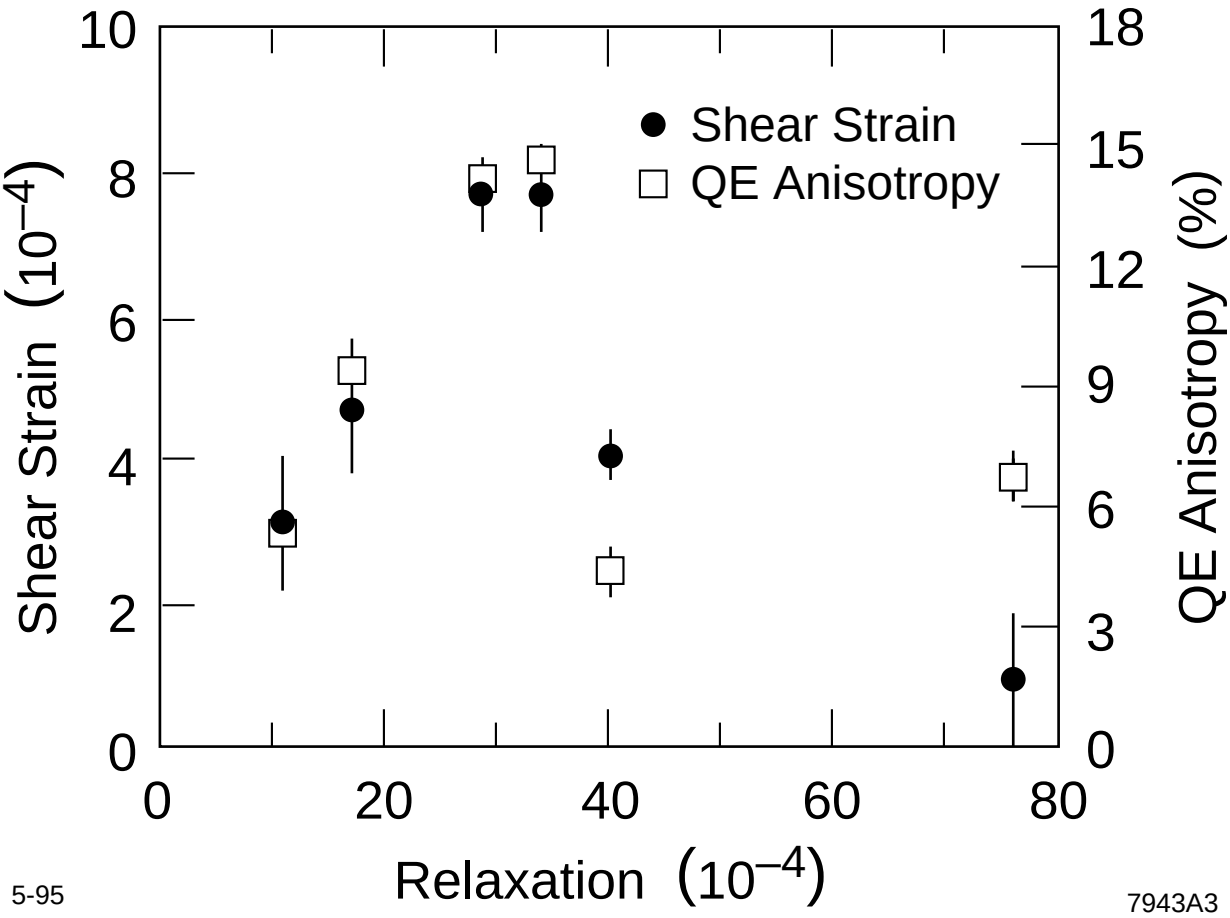
Shear Strain
QE Anisotropy
Shear Strain (10^{-4})
QE Anisotropy (%)
Relaxation (10^{-4})
0
2
4
6
8
10
0
3
6
9
12
15
18
0
20
40
60
80
5-95
7943A3

Figure 3: